Available online at www.sciencedirect.com
SCIENCE DIRECT®
Journal of Colloid and Interface Science 297 (2006) 122–129
JOURNAL OF Colloid and Interface Science
www.elsevier.com/locate/jcis

Preparation of siloxy focal dendron-protected TiO_2 nanoparticles and their photocatalysis

Yuko Nakanishi [a], Toyoko Imae [a,b,*]

[a] *Graduate School of Science, Nagoya University, Chikusa, Nagoya 464-8602, Japan*
[b] *Research Center for Materials Science, Nagoya University, Chikusa, Nagoya 464-8602, Japan*

Received 5 May 2005; accepted 14 October 2005

Available online 9 November 2005

Abstract

TiO_2 nanoparticles were synthesized at ∼0 °C by hydrolyzing $[(CH_3)_2CHO]_4Ti$ in 1-propanol solutions of poly(amido amine) dendrons with a siloxy focal point and long alkyl chain spacers. Transmission electron microscopic photographs showed that TiO_2 nanoparticle was 1–5 nm in size and protected by dendrons, when prepared at a mixing ratio 1:10 of Ti ion and dendron. At higher contents of Ti ion, TiO_2 nanoparticles aggregated up to a maximum size of 90 nm, depending on the dendron generation (first to third). It was confirmed from X-ray photoelectron spectroscopy that Si–O–Ti covalent bond was formed in dendron-protected TiO_2 nanoparticles. The ability of dendron-protected TiO_2 nanoparticles as a photocatalyst for the photodegradation of 2,4-dichlorophenoxyacetic acid was higher than that of nonprotected nanoparticle and superior at higher generation. It was suggested that the dendrons protecting TiO_2 nanoparticle have enough void volume to conserve guest molecules and behave effectively as a reservoir of guest molecules.

Keywords: TiO_2; Nanoparticle; Dendron; Siloxy focal dendron; Long alkyl chain spacer; Poly(amido amine) dendron; Transmission electron microscopy; X-ray photoelectron spectroscopy; Photodegradation; 2,4-Dichlorophenoxyacetic acid; Photocatalysis

1. Introduction

Titanium dioxide has attracted much attention in the fields of photocatalysis and solar system [1,2], and basic researches have been reported toward their applications [3–12]. To acquire effective photocatalysts in decomposing pollutants in air and solutions, TiO_2 materials must be fabricated with large surface areas and greatly porous structures (preferred in nanoscale) in order to contact efficiently with pollutants. So far, large numbers of studies have been done to achieve various TiO_2 nanomaterials with large surface area such as thin films [3,5–8,11,12], nanotubules [4,9] and nanoparticles [13–23], consisting of nanocrystals. Especially, TiO_2 nanoparticles, which were dispersed in water, have the application to the detoxification of water pollution environment [24–28]. However, such system is not sufficiently established, since the dispersibility of TiO_2 nanoparticles in water is low [29] because of the hydrophobicity of nanoparticles.

Size of TiO_2 nanoparticles is essential for the stable dispersion of nanoparticles in medium. The TiO_2 nanoparticles with small sizes were synthesized by the oxidation of $TiCl_4$ [13–15,19] or the hydrolysis of tetraisopropyl orthotitanate (titanium isopropoxide) [16–18,20–24] and utilized for the examination of photophysical property [13], relaxation dynamics [14], and photoluminescence [15]. The synthesized and commercial TiO_2 nanoparticles were also used for the photocatalytic degradation of phenol [20], surfactant [24], dyes [25–27], and 2,4-dichlorophenoxyacetic acid [28]. Using medium-soluble protectors enables the preparation of medium-dispersible TiO_2 nanoparticles. Dodecylbenzenesulfonate-capped TiO_2 nanoparticles were synthesized and their optical and photochemical properties were examined in nonaqueous solvents [22].

Poly(amido amine) (PAMAM) dendrimers are a useful protector and stabilizer for water-dispersible metal nanoparticles [30]. In the previous work, we synthesized water-dispers-

* Corresponding author. Fax: +81 52 789 5912.
E-mail address: imae@nano.chem.nagoya-u.ac.jp (T. Imae).

0021-9797/$ – see front matter
doi:10.1016/j.jcis.2005.10.017

ible TiO_2 nanoparticles by using forth generation (G4) PAMAM dendrimers as a protectant [30]. The resultant dendrimer-protected TiO_2 nanoparticles stably dispersed in water. These nanoparticles were more active in water as a photocatalyst than TiO_2 nanoparticles without protector. On the other hand, the interaction of PAMAM dendrimer with metal or metal oxide nanoparticles is not necessarily strong. Amine-terminated PAMAM dendrimers covering a gold nanoparticle were easy replaced by dodecanethiol [30].

In order to prepare water-dispersible TiO_2 nanoparticles protected by advantageous dendritic polymer, in the present work, TiO_2 nanoparticles were synthesized by using a dendron protector, which has a siloxy focal point and long alkyl (hexyl, C6) chain spacers. Then the siloxy group is able to form covalent bond with TiO_2 nanoparticles through Si–O–Ti bond. The photocatalytic activity of dendron-protected TiO_2 nanoparticles in water was also examined and compared with that of dendrimer-protected TiO_2 nanoparticles.

2. Experimental

2.1. Reagents

3-Aminopropyl triethoxysilane was purchased from Aldrich Chemical Co. Methylacrylate, hexamethylene diamine, tetraisopropyl orthotitanate ($[(CH_3)_2CHO]_4Ti$), and tetraethyl orthosilicate (TEOS) were products from Tokyo Chemical Industry Co. 2,4-Dichlorophenoxyacetic acid (2,4-DPA) was obtained from MERK Achuchardt. The other reagents were of analytical grade. The chemicals were used without further purification. Ultrapure water (Millipore Milli-Q) was utilized throughout all experiments.

2.2. Synthesis of dendrons

Generation 1–3 (G1–G3) siloxy focal C6-PAMAM dendrons with amine terminals were synthesized from 3-aminopropyl triethoxysilane by repeating two steps of Michael addition and amidation, as described elsewhere [32]. On a Michael addition reaction, methylacrylate in methanol was added dropwise into a methanol solution of 3-aminopropyl triethoxysilane or full-generation dendron under nitrogen atmosphere. On an amidation reaction, hexamethylene diamine in methanol was added dropwise to a methanol solution of a Michael addition product (a half-generation dendron) under nitrogen atmosphere. Both reaction mixtures were stirred at room temperature for one day. Then the excess solvent and unreacted compounds were removed by vacuum distillation to give a yellow oil-like product.

2.3. Synthesis of nanoparticles

TiO_2 nanoparticles were prepared by the hydrolysis of $[(CH_3)_2CHO]_4Ti$ in 1-propanol. Liquid $[(CH_3)_2CHO]_4Ti$ (0.01 cm^3) and G1–G3 siloxy focal C6-PAMAM dendron were mixed, at various mixing ratios of Ti ion and dendron, in 1-propanol (5 cm^3) cooled at ∼0 °C. The mixed solution was dropwise added, under vigorous stirring, to water (10 cm^3) maintained at ∼0 °C. The dialysis by water (1000 cm^3) in a Viscose membrane (presoaked in water and then thoroughly rinsed prior to use) was repeated for two days in order to remove the unreacted chemicals. For comparison, TiO_2 nanoparticles were also prepared in absence of protective dendron or in addition of TEOS instead of dendron.

2.4. Measurements

Microscopic observation was performed on a Hitachi H-7000 transmission electron microscope (TEM) equipped with a CCD camera attachment, operating at 100 kV. Fourier transform infrared (IR) absorption spectra in the region of 4000–700 cm^{-1} were recorded on a Bio-Rad FTS 575C instrument. X-ray photoelectron spectroscopic (XPS) measurement was carried out on a Shimazu ESCA-3300 spectroscopy. The X-ray source (MgK_α, 1253.6 eV) was operated at 10 kV and 30 mA. Specimens were exposed in argon for overnight to purge contamination. Specimens were prepared on substrates by casting a droplet of solutions and drying. The substrates were a CaF_2 window for IR spectroscopy and a copper grid coated with a thin carbon film for TEM and XPS. Fluorescence was measured on a HITACHI F-4010 fluorometer with a quartz cell (10 mm path). Ultraviolet-visible absorption spectra were measured on a Shimazu UV 2200 spectrometer using a quartz cell (10 mm path). The absorbance was calibrated by the background absorbance of the solvent. All measurements were performed at room temperature (∼25 °C).

2.5. Photodegradation and solubility

Aqueous suspensions of TiO_2 nanoparticles containing 2,4-DPA (3.0 mM) were photoirradiated by using a HOYA EX250 UV light source with a 250 W Hg lamp (below 320 nm). The degradation of 2,4-DPA was monitored by the intensity $I_{357\,\mathrm{nm}}(t)$ of an emission band at 357 nm, at an irradiation time t, which was normalized by the intensity $I_{357\,\mathrm{nm}}(0)$ at zero time. The excitation wavelength was at 254 nm.

Solubility was determined by shaking aqueous dendron solutions with excess powder of 2,4-DPA for two days. After filtering out the insoluble powder, ultraviolet-visible absorbance of 2,4-DPA was measured and the solubility per dendron was calculated by using an extinction coefficient of 2,4-DPA.

3. Results and discussion

3.1. Morphology and size distribution of TiO_2 nanoparticles

Morphologies of TiO_2 nanoparticles prepared with G1 dendron at 1:1 and 1:10 mixing ratios of Ti ion and dendron ($[Ti^{4+}]$:[dendron]) were observed on a TEM. As seen in Fig. 1a, TiO_2 nanoparticles at 1:1 were spherical particles with sizes less than 90 nm as well as those without dendrons (Fig. 1c). On the other hand, TiO_2 nanoparticles prepared at 1:10 were fairly small (<5 nm) and surrounded by dendrons (Fig. 1b). TiO_2 nanoparticles were also synthesized at different mixing ratios of Ti ion and G3 dendron. Their TEM photographs are

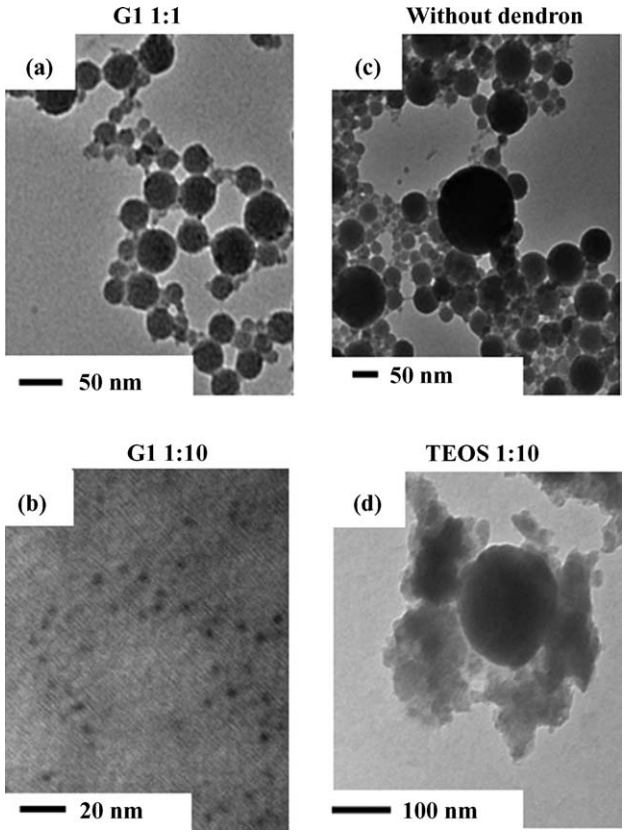

Fig. 1. TEM photographs of TiO_2 nanoparticles: (a) with G1 dendron at a 1:1 mixing ratio, (b) with G1 dendron at 1:10, (c) without dendron, (d) with TEOS at 1:10.

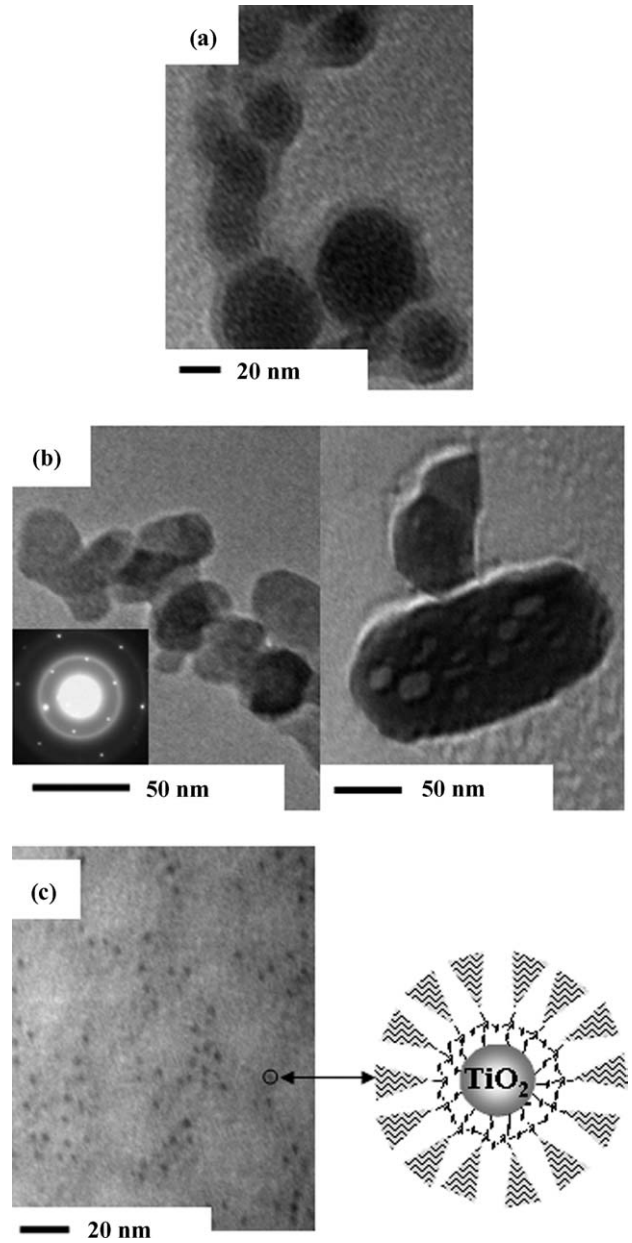

Fig. 2. TEM photographs of TiO_2 nanoparticles protected with G3 dendron. Mixing ratio: (a) 1:0.01, (b) 1:1, (c) 1:10. A dendron-protected TiO_2 nanoparticle is schematically illustrated.

shown in Fig. 2. TiO_2 nanoparticles prepared at a mixing ratio of 1:0.01 (Fig. 2a) were spheres (average diameter ∼60 nm) covered with thin layer (thickness ∼10 nm). At a mixing ratio of 1:1, the dominant structure of TiO_2 nanoparticles was spherical (diameter 20–30 nm), and the tabular TiO_2 nanoparticles (average diameter ∼100 nm) coexisted at a content of less than 5%, as seen in Fig. 2b. The electron diffraction pattern, which was inset in Fig. 2b, presented some diffraction spots with Debye–Scherrer rings, indicating crystallinity of nanoparticles. The morphology of TiO_2 nanoparticles at a mixing ratio of 1:0.1 (data is not shown) was similar to that at the ratio of 1:1. Similar TiO_2 nanoparticles were obtained for a case of Ti ion and G2 dendron at 1:1 (data is not shown). When the mixing ratio of Ti ion to G3 dendron is 1:10, small spherical TiO_2 particles (diameter 1–5 nm) (Fig. 2c) were covered with the network of the dendrons, similarly with particles prepared with G1 dendrons at 1:10 in Fig. 1b.

Histograms of size distribution (200 samples) of particles prepared with G1–G3 dendrons are shown in Figs. 3 and 4 for mixing ratios of 1:1 and 1:10, respectively. The sizes of TiO_2 nanoparticles were 10–90, 15–90, and 10–35 nm for G1, G2, and G3 dendrons, respectively, at a mixing ratio of 1:1 and 1–4 and 1–5 nm for G1 and G3 dendrons, respectively, at 1:10. Average diameters are listed in Table 1. It can be revealed that the sizes of TiO_2 nanoparticles prepared with dendrons decrease with increasing the generation of dendrons and with decreasing the mixing ratio, that is, increasing the fraction of dendron. The growth and the aggregation between TiO_2 nanoparticles may be prevented due to the protection by dendron-coating. It should be noticed that the suspensions of dendron-coated TiO_2 nanoparticles in water were viscous and opalescent but did not precipitate even over one month, different from the naked TiO_2 nanoparticles which precipitated within a couple of days.

3.2. *Binding of dendrons on TiO_2 nanoparticles*

On XPS analysis, an O_{1s} signal for TiO_2 nanoparticles prepared in a G3 dendron solution at a mixing ratio of 1:1 presented a band at 533.2 eV and a shoulder located on the lower binding energy side, as shown in Fig. 5. Both a band and a shoulder were observed for all dendron-coated TiO_2 nanoparti-

cles. The decomposed O_{1s} spectrum of the TiO_2 nanoparticles resulted in the second and third bands at binding energies of 532.5 and 531.0 eV. While the first (533.2 eV) and third bands are assigned to O–Si and O–Ti species, respectively, the second band is in agreement with the reported O_{1s} binding energy of the Si–O–Ti species [33,34], which reflects the bonding of siloxy focal dendron on a TiO_2 nanoparticle.

IR spectra of TiO_2 nanoparticles prepared with G1–G3 dendrons at a mixing ratio of 1:1 displayed, in common, characteristic bands of the dendrons at 2926 (ν_{as,CH_2}), 2854 (ν_{s,CH_2}), 1674 (amide I), 1598 (amide II), 1454 (σ_{CH_2}) and 1349 cm^{-1} (amide III). Both IR spectroscopic and XPS results indicate the coexistence and covalent bonding of TiO_2 nanoparticles and dendrons.

3.3. Composition of dendron-protected TiO_2 nanoparticles

It was confirmed from XPS that both titanium and nitrogen which originated from TiO_2 and dendron, respectively, exist in the dendron-protected TiO_2 nanoparticles at the mixing ra-

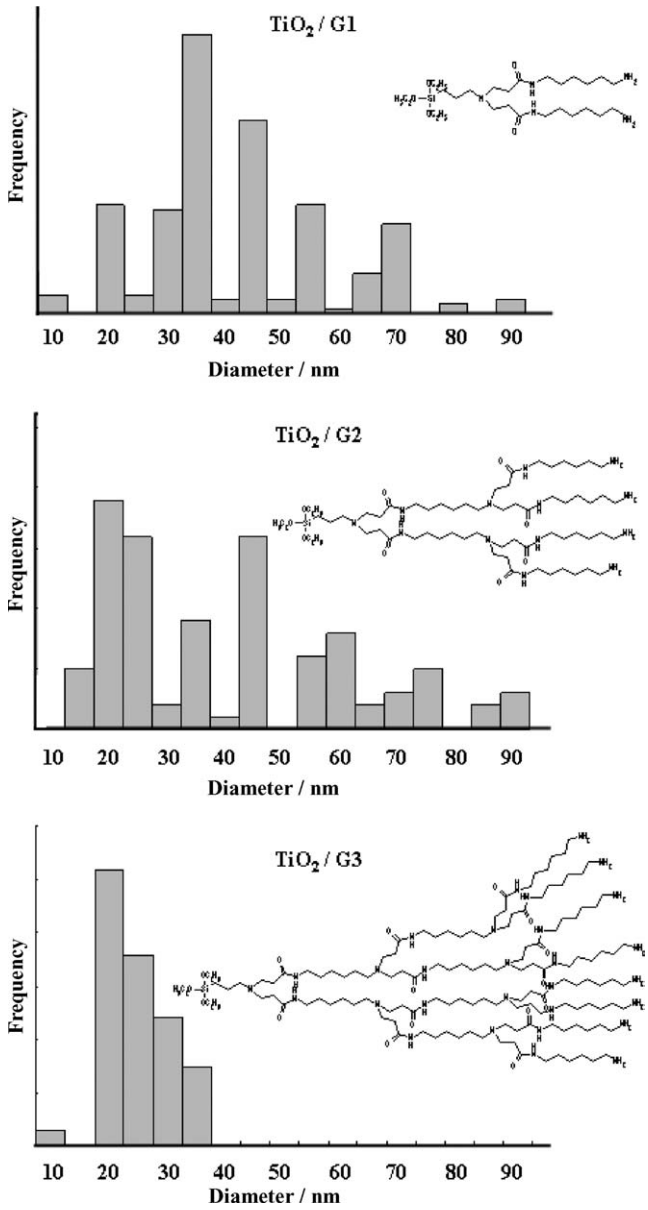

Fig. 3. Size histograms of TiO_2 nanoparticles protected with dendrons. Mixing ratio of Ti and dendron is 1:1. Chemical structures of dendrons are included.

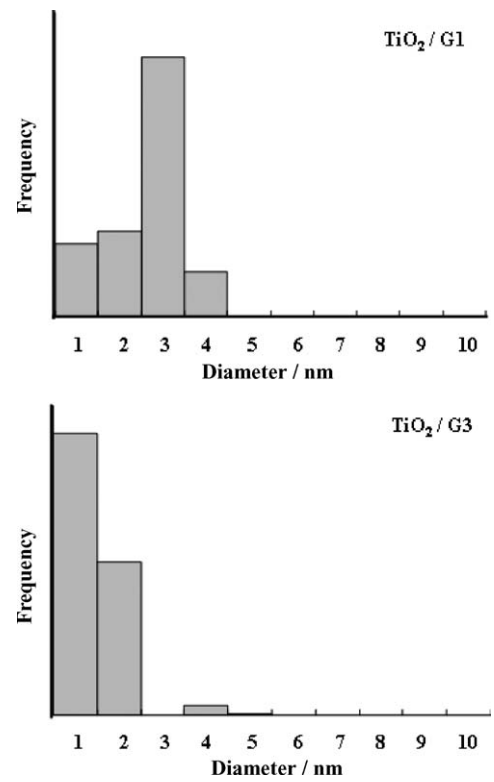

Fig. 4. Size histograms of TiO_2 nanoparticles protected with dendrons. Mixing ratio of Ti and dendron is 1:10.

Table 1
Size and composition of TiO_2 nanoparticles protected with dendrons

Mixing ratio [Ti^{4+}]:[dendron]	Nanoparticle	Average diameter of TiO_2 nanoparticle (nm)	[Ti]:[dendron]	[Ti]:[Si–O–Ti]	Binding mode		
					Si–O–Ti in TiO_2 [I]	Si–O–Ti on TiO_2 [II]	O–Si [III]
1:0	TiO_2	49.2 ± 1.6					
1:1	TiO_2/Gl	47.8 ± 1.4	1:0.05	1:0.03	4.7	1.0	3.4
1:1	TiO_2/G2	40.1 ± 3.6	1:0.04	1:0.04	−0	1.0	0.1
1:1	TiO_2/G3	24.7 ± 3.6	1:0.02	1:0.006	−0	1.0	2.2
1:10	TiO_2/Gl	3.06 ± 2.5	1:3	1:0.5	−0	1.0	5.1
1:10	TiO_2/G3	2.63 ± 2.0	1:0.04	1:0.02	−0	1.0	1.4

tios 1:1 and 1:10, as seen in Figs. 6 and 7, respectively. The $Ti_{2p_{1/2}}$, $Ti_{2p_{3/2}}$ and N_{2s} spin-orbital splitting photoelectrons for all nanoparticles were located at the binding energies of 465.3, 459.4, and 401.4 eV, respectively. The peak separation of 5.9 eV between the $Ti_{2p_{1/2}}$ and $Ti_{2p_{3/2}}$ signals is in agreement with a value of 5.92 eV in the literature [33,34]. The area ratio of $Ti_{2p_{3/2}}$ and N_{2s} signals was evaluated, and, then, the component ratio of dendron to Ti was calculated for TiO_2 nanoparticles prepared with G1, G2, and G3 dendrons at a mixing ratios of 1:1 and 1:10. Moreover, the number ratio of Si–O–Ti bond to Ti was obtained from areas of $Ti_{2p_{3/2}}$ and O_{1s} (Si–O–Ti) peaks. Numerical values are listed in Table 1.

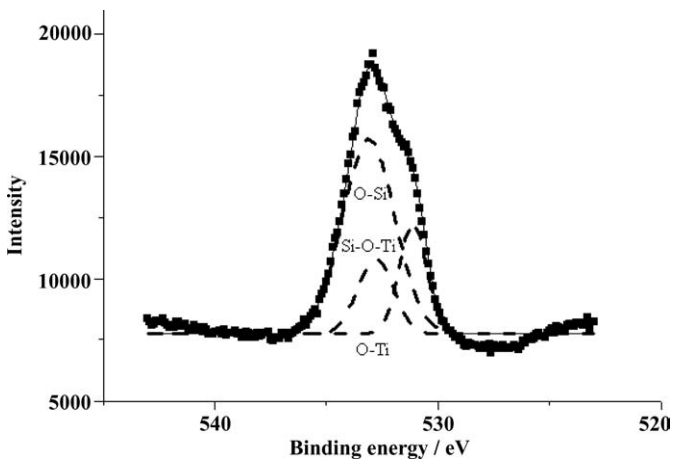

Fig. 5. An O_{1s} signal in an XPS for TiO_2 nanoparticles protected with G3 dendron at a mixing ratio of 1:1. The decomposition of its signal is drawn by broken lines.

At this moment, it was assumed that Si takes three binding modes as follows: (I) Si–O–Ti bond in interior of TiO_2 nanoparticles, (II) Si–O–Ti bond on surface of TiO_2 nanoparticles, (III) O–Si bond in and between dendrons, which were illustrated in Fig. 8. Since a fraction of mode I + II to Ti is evaluated as described above, a fraction of mode III could be calculated by subtracting a fraction of mode I + II from a fraction of dendron. Fractions of mode I and II were calculated as below. At first, a number of Ti in TiO_2 nanoparticle was estimated from the density of TiO_2 particle (3.893 g/cm^3) and an average diameter of TiO_2 nanoparticle in Table 1. Second, a number of dendrons, which are able to attach on the surface of TiO_2 nanoparticle, was calculated on the basis of the molecular size of dendron. The number ratio of Ti in TiO_2 nanoparticle and dendron on a TiO_2 nanoparticle is a fraction of binding mode II. Subtraction of a mode II fraction from a mode I + II fraction corresponds to a mode I fraction. Contribution ratio of three binding modes is listed in Table 1.

It should be noted that, commonly for all cases examined, the fraction of dendron to Ti is fairly small in comparison with the initial feed fraction. Many free dendrons might pass away during dialysis. Dendrons engaged upon TiO_2 nanoparticles are almost located on the surface of nanoparticles except a case of nanoparticles protected by G1 dendron at a 1:1 mixing ratio. In the case of nanoparticles protected by dendron at a 1:1 mixing ratio, large TiO_2 nanoparticles (up to 90 nm) are aggregates of small primitive TiO_2 nanoparticles (a few nm in diameter). Then the finding of the mode I may imply the existence of dendrons embedded within aggregates during their formation. Such mode was evaluated only in the TiO_2/G1 dendron mixture at a

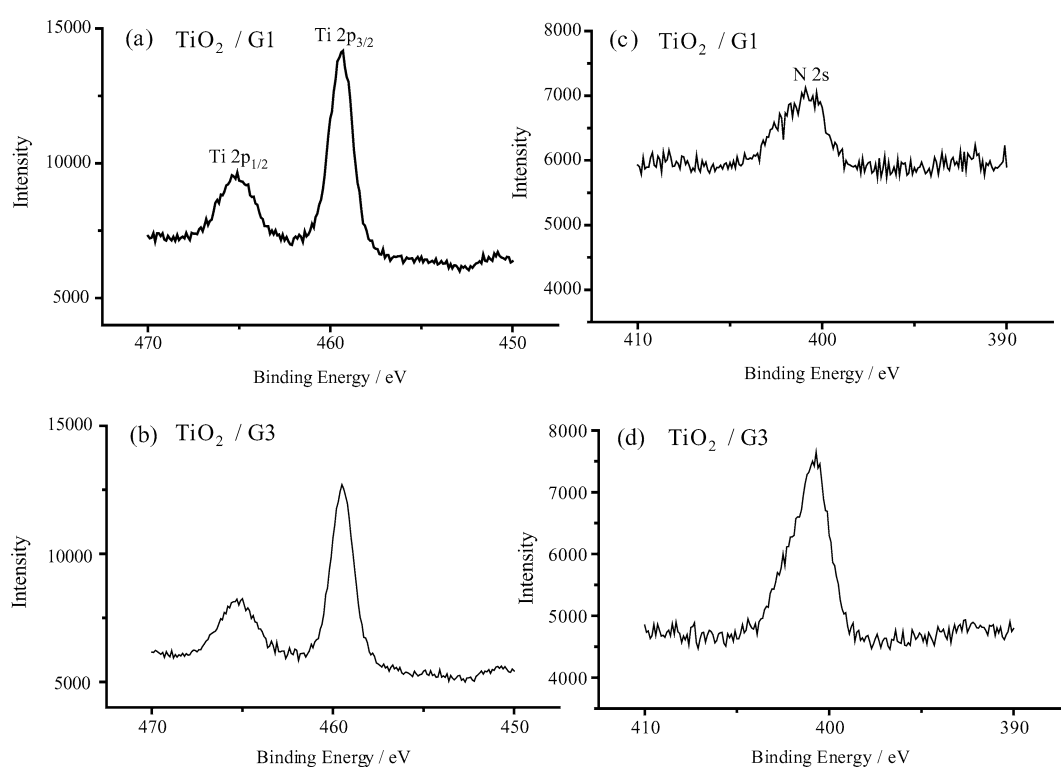

Fig. 6. Ti_{2p} and N_{2s} signals in an XPS for TiO_2 nanoparticles protected with dendron. (a), (b) Ti_{2p}; (c), (d) N_{2s}. Mixing ratio of Ti and dendron is 1:1.

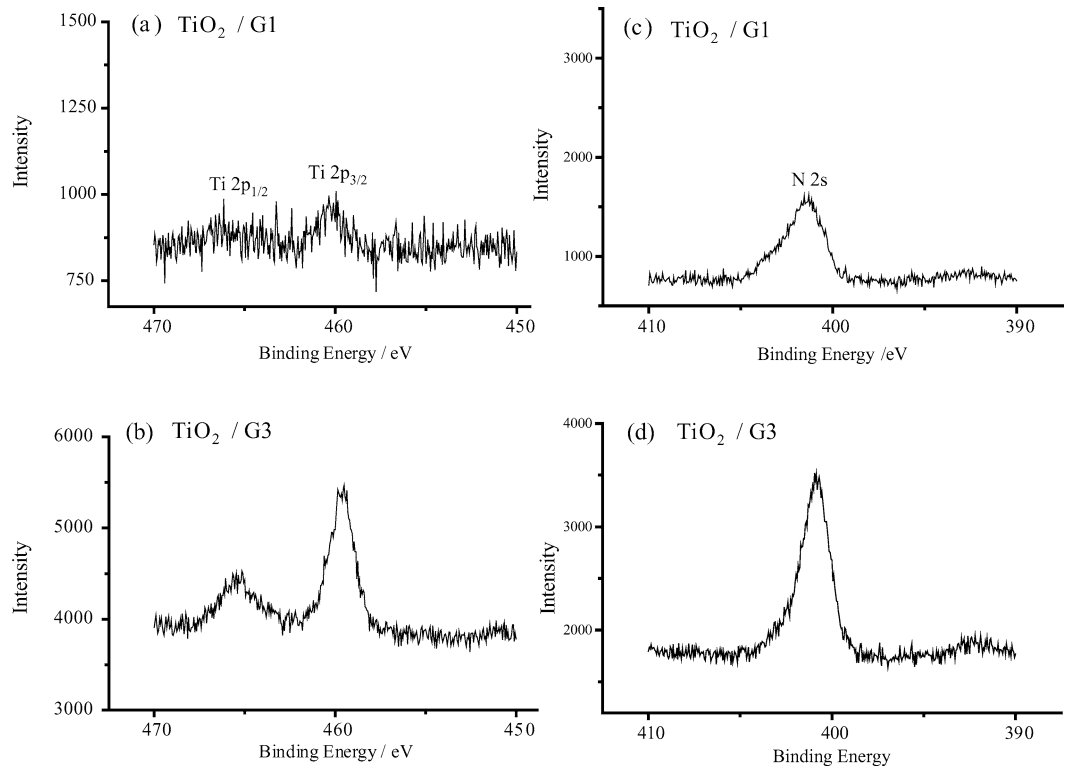

Fig. 7. Ti_{2p} and N_{2s} signals in an XPS for TiO_2 nanoparticles protected with dendron. (a), (b) Ti_{2p}; (c), (d) N_{2s}. Mixing ratio of Ti and dendron is 1:10.

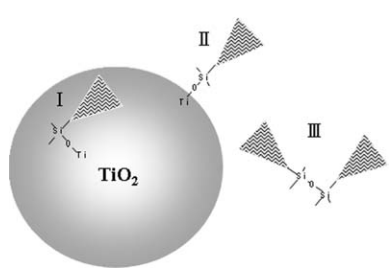

Fig. 8. Three binding modes of Si: (I) Si–O–Ti bond in interior of TiO_2 nanoparticle, (II) Si–O–Ti bond on surface of TiO_2 nanoparticle, (III) O–Si bond.

mixing ratio of 1:1. Small dendron should be easy ingested in the aggregates.

If exclude a case of protection by G2 dendron at 1:1, O–Si bond connected to TiO_2 nanoparticles are rather less amount than O–Si bond free from the binding with TiO_2 nanoparticles, which take bonds in the mode III. This means that each of three ethoxysilane groups at focal point of the dendron forms a Si–O–Si bond besides a Si–O–Ti bond or is as it is.

3.4. Optimum condition of nanoparticle formation

It was confirmed that the mixing ratio played an important role in the formation of TiO_2 nanoparticles. In the case of G1 dendron, larger TiO_2 nanoparticle, average size (∼50 nm) of which was not different from that of the naked TiO_2 nanoparticle, was synthesized at a mixing ratio of 1:1 (compare Figs. 1a and 1c). On the other hand, TiO_2 nanoparticle at a mixing ratio of 1:10 was 1–4 nm in diameter, and it seemed to exist in the mesh network of dendron (see Fig. 1b). In the case of G3 dendron, the tendency of TiO_2 nanoparticle formation was similar to the case of G1 dendron. G1 dendrons at a mixing ratio of 1:1 were covalent-bonded with TiO_2 nanoparticles not only on their surface but also at the embedded situation into aggregates of nanoparticles. On the other hand, at higher dendron content and generation, dendrons covalently bonded only on the surface of TiO_2 nanoparticles.

Additionally, dendron generation was also important in the formation of TiO_2 nanoparticles. At higher dendron generation, smaller TiO_2 nanoparticles were formed. Especially, branched chains in the dendron were expected to play a remarkable role from the following result. The synthesis of TiO_2 nanoparticles protected by dendrons was compared with that prepared in the presence of tetraethyl orthosilicate (TEOS), where both dendron and TEOS have a common reactive moiety, silicate. As seen in Fig. 1d, TiO_2 nanoparticles prepared with TEOS were larger in size (∼150 nm in diameter) than those with dendrons. This suggests that not only the Ti/dendron mixing ratio and the dendron generation but also the branched structure in the dendron were especially important as a protector in the formation of TiO_2 nanoparticles.

3.5. Photodegradation of 2,4-dichlorophenoxyacetic acid in aqueous suspensions of TiO_2 nanoparticles

The photocatalytic property of TiO_2 nanoparticles protected by G1 and G3 C6-PAMAM dendron at a mixing ratio of 1:10

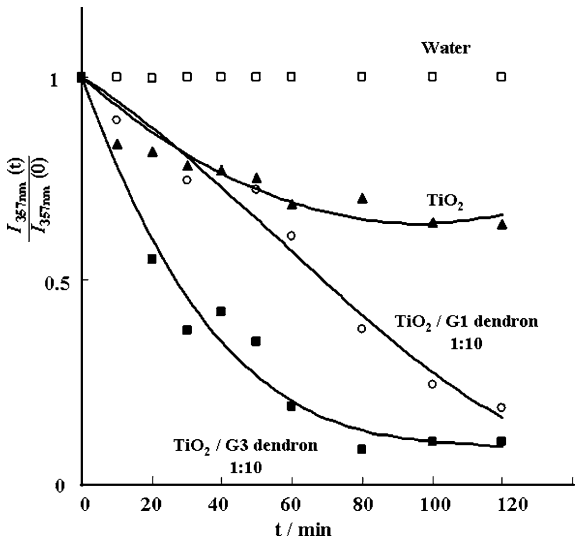

Fig. 9. Degradation degree of 2,4-DPA monitored by the intensity $I_{357}(t)$ of a fluorescence emission band of 357 nm at an irradiation time t normalized by the intensity $I_{357}(0)$ at zero time.

was investigated for the photodegradation of 2,4-DPA. The normalized intensity of an emission band at 357 nm in fluorescence spectra of 2,4-DPA under the irradiation of UV light decreased with time, as seen in Fig. 9, where the results of photodegradation in water and an aqueous suspension of the naked TiO_2 nanoparticles were also included. It is apparent that the resulting loss of fluorescence emission is due to the degradation of 2,4-DPA, because such loss of emission occurred even in the naked TiO_2 suspension. The dendron-protected TiO_2 nanoparticles are more efficient as a photocatalyst than the naked TiO_2 nanoparticles. It is caused by the character of dendron, which has not only the ability as a protector but also the host ability against small organic guest molecules on the photocatalysis of TiO_2 nanoparticles. It is expected that a guest molecule is trapped in the interior of a dendron before photodegradation. In other words, the dendrimer behaved as a reservoir of 2,4-DPA. Similar remark was also obtained in a case of dendrimer-protected TiO_2 nanoparticles [31].

The difference of efficiency between TiO_2 nanoparticles protected with G1 and G3 dendrons should be caused by the trapping volume around TiO_2 nanoparticles, especially, by the number of 2,4-DPA coming close on the surface of TiO_2 nanoparticles. It could be expected that the host ability of G3 dendron is higher than that of G1 dendron due to larger molecular volume. Additionally, the degradation process was considered by a first-order kinetics of $-\mathrm{d}[2,4\text{-DPA}]/\mathrm{d}t = kt$. The rate constants were evaluated by fitting the calculated curves to the observed emission intensity decrease. Solid lines in Fig. 9 show the optimum fitting curves. The obtained rate constants were $k = 3.2 \times 10^{-3}\ \mathrm{min}^{-1}$ for the naked TiO_2 nanoparticles and $k = 13 \times 10^{-3}$ and $29 \times 10^{-3}\ \mathrm{min}^{-1}$ for TiO_2 nanoparticles protected by G1 and G3 dendrons, respectively. The decomposition rate of 2,4-DPA on TiO_2 nanoparticles protected by G3 dendron was nine times higher than that on bare nanoparticles and two times higher than that on nanoparticles protected by G1 dendron.

Table 2
Rate constants of the first order reaction on photodegradation of 2,4-DPA in nanoparticle suspensions and solubility of 2,4-DPA in dendritic polymers

Dendritic polymer	Rate constant (10^{-3} min^{-1})	Solubility*
No.	3.2	
G4.5 PAMAM dendrimer	9.8	5.3
Gl C6-PAMAM dendron	13	8.5
G3 C6-PAMAM dendron	29	18.8

* Number of the solubilized 2,4-DPA per polymer molecule.

Solubility of 2,4-DPA in G1 and G3 dendrons was examined in water, and 8.5 and 18.8 2,4-DPA molecules were practically encapsulated in G1 and G3 dendrons, respectively. Two times larger solubility in G3 dendron than in G1 dendron is the same tendency as that of decomposition rate. In consequence, it can be supported that the difference of photodegradation efficiency between TiO_2 nanoparticles was caused by the host ability of dendrons for guest molecule. This effect should be related to the length of alkyl chain in dendron. In other words, the void volume of a G1 or G3 dendron is large enough to conserve guest molecules in the dendron.

The kinetics of photodegradation was also examined on TiO_2 nanoparticles that were protected by commercially available G4.5 PAMAM dendrimer [31]. The rate constant of the first-order degradation kinetics was $9.8 \times 10^{-3}\ \mathrm{min}^{-1}$ and the solubility of 2,4-DPA was only 5. As compared in Table 2, these numbers are smaller than cases of G3 and G1 dendrons. This originates in the fact that the commercial PAMAM dendrimer with ethylene spacers has less void volume or less host ability.

4. Conclusions

In this study, dendrons were used as a stabilizer for TiO_2 nanoparticles with an expectation of the increasing stability of nanoparticles in water. The synthesis of dendron-protected TiO_2 nanoparticles was performed by the hydrolysis of $[(CH_3)_2CHO]_4Ti$ in a cold aqueous solution of dendrimer. The morphology of dendron-protected TiO_2 nanoparticles was dependent on the dendron generation and especially the mixing ratio of Ti ion and dendron. The sizes of dendron-protected TiO_2 nanoparticles were 10–90 nm at a ratio ($[Ti^{4+}]$:[dendron]) of 1:1, depending on the dendron generation. The sizes were close to that of bare TiO_2 nanoparticles. At the mixing ratio of 1:10, the particle size was 1–5 nm. The Si–O–Ti covalent bond was detected in all dendron-protected TiO_2 nanoparticles. At a mixing ratio of 1:1, G1 dendrons not only existed on the surface of TiO_2 nanoparticles but also were embedded in aggregates of nanoparticles. On the other hand, at 1:10, they located only on the surface of TiO_2 nanoparticles. The photodegradation of 2,4-dichlorophenoxyacetic acid was more reactive in an aqueous suspension of dendron-protected TiO_2 nanoparticles than in a suspension of naked TiO_2 nanoparticles. It was concluded that dendrons reinforce the photocatalytic activity of TiO_2 nanoparticles, besides the stabilization of the nanoparticles, by means of their trapping ability. The photodegradation ability and doping ability of C6-PAMAM dendron-protected nanoparticles were more excellent than that of commercial PAMAM dendrimer.

Acknowledgments

We acknowledge Dr. Ryo Sasai of Nagoya University for his kind permission and guidance of XPS measurement. This work was supported by a Grant-in-Aid for Scientific Research (B) (15350067) from the Ministry of Education, Culture, Sports, Science, and Technology (MEXT) of the Japanese Government.

References

[1] A. Fujishima, K. Honda, Nature 238 (1972) 37.
[2] B. O'Regan, M. Grätzel, Nature 353 (1991) 737.
[3] B.L. Bischoff, M.A. Anderson, Chem. Mater. 7 (1995) 1772.
[4] B.B. Lakshmi, P.K. Dorhout, C.R. Martin, Chem. Mater. 9 (1997) 857.
[5] S.D. Burnside, V. Shklover, C. Barbe, P. Comete, F. Arendse, K. Brooks, M. Grätzel, Chem. Mater. 10 (1998) 2419.
[6] T. Tatsuma, S. Tachibana, T. Miwa, D.A. Tryk, A. Fujishima, J. Phys. Chem. B 103 (1999) 8033.
[7] N. Sakai, A. Fujishima, T. Watanabe, K. Hashimoto, J. Phys. Chem. B 105 (2001) 3023.
[8] S. Nakade, S. Kambe, T. Kitamura, Y. Wada, S. Yanagida, J. Phys. Chem. B 105 (2001) 9150.
[9] D.-S. Seo, J.-K. Lee, H. Kim, J. Cryst. Growth 229 (2001) 428.
[10] Y. Ishikawa, Y. Matsumoto, Electrochem. Acta 46 (2001) 2819.
[11] B.H. Sohn, H.T. Kim, K. Char, Langmuir 18 (2002) 7770.
[12] T. Tatsuma, W. Kubo, A. Fujishima, Langmuir 18 (2002) 9632.
[13] N. Serpone, D. Lawless, R. Khairutdinov, J. Phys. Chem. 99 (1995) 16646.
[14] N. Serpone, D. Lawless, R. Khairutdinov, E. Pelizzetti, J. Phys. Chem. 99 (1995) 16655.
[15] Y. Liu, R.O. Claus, J. Am. Chem. Soc. 119 (1997) 5273.
[16] T. Moritz, J. Reiss, K. Diesner, D. Su, A. Chemseddine, J. Phys. Chem. B 101 (1997) 8052.
[17] A. Zaban, T.S. Aruna, S. Tirosh, A.B. Gregg, Y. Mastai, J. Phys. Chem. B 104 (2000) 4130.
[18] N.H. Ghosh, S. Adhikai, Langmuir 17 (2001) 4129.
[19] D.H. Jang, S.K. Kim, Mater. Res. Bull. 36 (2001) 627.
[20] L. Znaidi, R. Seraphimova, J.F. Bocquet, C. Colbeau-Justin, C. Pommier, Mater. Res. Bull. 36 (2001) 811.
[21] A. Dawson, V.P. Kamat, J. Phys. Chem. B 105 (2001) 960.
[22] G. Ramakrishna, N.H. Ghosh, Langmuir 19 (2003) 505.
[23] G. Oskam, A. Nellore, L.A. Penn, C.P. Searson, J. Phys. Chem. B 107 (2003) 1734.
[24] J. Zhao, H. Hidaka, A. Takamura, E. Pelizzetti, N. Serpone, Langmuir 9 (1993) 1646.
[25] T. Zhang, T. Oyama, S. Horikoshi, H. Hidaka, J. Zhao, N. Serpone, Sol. Energy Mater. & Sol. Cells 73 (2002) 287.
[26] C. Chen, X. Li, W. Ma, J. Zhao, H. Hidaka, N. Serpone, J. Phys. Chem. B 106 (2002) 318.
[27] C. Chen, W. Zhao, J. Li, J. Zhao, H. Hidaka, N. Serpone, Environ. Sci. Technol. 36 (2002) 3604.
[28] S. Horikoshi, F. Houjo, N. Serpone, H. Hidaka, J. Photochem. Photobiol. A Chem. 159 (2003) 289.
[29] T. Imae, K. Muto, S. Ikeda, Colloid. Polym. Sci. 269 (1991) 43.
[30] T. Imae, K. Funayama, Y. Nakanishi, K. Yoshii, in: H.S. Nalwa (Ed.), Encyclopedia of Nanoscience and Nanotechnology, in: Am. Sci. Pub., vol. 3, 2004, pp. 685–701, and literatures cited in there.
[31] Y. Nakanishi, T. Imae, J. Colloid Interface Sci. 285 (2005) 158.
[32] O. Yemul, M. Ujihara, T. Imae, Trans. Mater. Res. Soc. Jpn. 29 (2004) 165.
[33] B. Erdem, A.R. Hunsicker, W.G. Simmons, D.E. Sudol, L.V. Dimonie, S.M. El-Aasser, Langmuir 17 (2001) 2664.
[34] Y. Masuda, S.W. Seo, K. Koumoto, Langmuir 17 (2001) 4876.